OLYMPUS

THESE ARE NOT **COFFEE BEANS.**

This is the cyanobacterium Chroococcus seen through a 60X X Line objective.

Image: © Håkan Kvarnström

Breaking barriers in optical performance.

See the truth
with Olympus X Line

DISCOVER MORE

X LINE

Contact your Olympus sales representative or visit **www.olympus-lifescience.com/108-xline** to learn more.

Received: 12 October 2020 | Accepted: 11 April 2021

DOI: 10.1111/jmi.13015

Journal of Microscopy RMS

ORIGINAL ARTICLE

Determination of the refractive index and wavelength-dependent optical properties of few-layer $CrCl_3$ within the Fresnel formalism

Shafaq Kazim[1] | **Roberto Gunnella**[1] | **Marco Zannotti**[2] | **Rita Giovannetti**[2] | **Tomasz Klimczuk**[3] | **Luca Ottaviano**[4,5]

[1] Physics Division, School of Science and Technology, University of Camerino, Camerino, MC, Italy

[2] Department of Chemistry, School of Science and Technology, University of Camerino, Camerino, MC, Italy

[3] Faculty of Applied Physics and Mathematics, Gdansk University of Technology, Gdansk, Poland

[4] Dipartimento di Scienze Fisiche e Chimiche (DSFC), Università degli Studi dell'Aquila, L'Aquila, Italy

[5] CNR-SPIN UoS L'Aquila, L'Aquila Via Vetoio 10 67100, Italy

Correspondence
Roberto Gunnella, Physics Division, School of Science and Technology, University of Camerino, 62032 Camerino MC, Italy.
Email: roberto.gunnella@unicam.it

Summary

Based on previous reports on the optical microscopy contrast of mechanically exfoliated few layer $CrCl_3$ transferred on 285 nm and 270 nm SiO_2 on Si(100), we focus on the experimental determination of an effective mean complex refractive index via a fitting analysis based on the Fresnel equations formalism. Accordingly, the layer and wavelength-dependent absorbance and reflectance are calculated. Layer and wavelength-dependent optical contrast curves are then evaluated demonstrating that the contrast is significantly high only around well-defined wavelength bands. This is validated a posteriori, by experimental UV-Vis absorbance data. The present study aims to show the way towards the most reliable determination of thickness of the 2D material flakes during exfoliation.

KEYWORDS

absorbance, Fresnel's equation, optical contrast, two-dimensional materials

1 | INTRODUCTION

Since the first isolation of graphene, the family of two-dimensional (2D) materials has been growing enormously.[1] Recent studies have reported that more than 1000 2D materials have been explored so far.[2] Interestingly, 2D physical concepts have been experimentally and theoretically proved in such materials since their discovery, as their atomic layers thinning drastically changes the properties of their bulk counterpart. In particular, as the layer thinning impacts the band structure, quantum confinement,[3,4] excitons,[5] topological order[6] and specific magnetic properties can emerge.[7,8] Recent discovery of ferromagnetism in monolayer CrI_3[7] boosted the research towards the 2D magnetism for spintronics.[9] After this ground-breaking discovery, the chromium trihalides group has received a renewed attention and significant work has been also focussed on $CrCl_3$.[10,11] Very little is reported on the optical properties of this novel class of 2D materials. Pollini and Spinolo determined the real part of refractive index on an evaporated thick film (several hundreds of nm) of $CrCl_3$, that is, 1.85 ± 0.1 at fixed $\lambda = 500$ nm with no information on the extinction coefficient part.[12]

There are plenty of experimental methods to prepare the thin layers of 2D materials like chemical vapour deposition,[13,14] chemical exfoliation,[15] physical

mechanical exfoliation[1,16,17] and electrochemical lithiation process,[8] but the mechanical exfoliation process is able to give the purest form of material due to the use of bulk crystal of respective materials.

In this regard, once mechanically exfoliated flakes are deposited onto dielectric substrates, it is well known that optical microscopy gives the way to distinguish the layer thickness of 2D materials by studying the Fresnel interference.[18–20] In particular, once the contrast is evaluated, using the Fresnel equations, the complex refractive index of the materials in their few layer phase can be determined.[21] To this respect, extensive studies are reported on the layer-dependent optical properties of graphene[20,22] and MoS_2.[23,24] The importance of optical contrast (O.C.) of $CrCl_3$ increases due to the reported Raman insensitivity on few layers.[25]

This article focusses on the determination of the layer-dependent optical properties (refraction index, reflectance and absorbance) of $CrCl_3$ by layer-dependent contrast measurements of exfoliated $CrCl_3$ supported on silica. We demonstrate independently from the characteristics of the illuminating source used in the microscope, that the use of broad-band light in the identification of few layer flakes of the material is preferable than the use of monochromatized light.

2 | NUMERICAL SIMULATION

Architecture of samples is made of three different materials: (1) flake, (2) silicon oxide and (3) silicon substrate. As reported in Figure 1, light, at a given incident angle θ is reflected and absorbed with different intensities by the two interfaces. The O.C. can be then quantified by using empirical relation as shown in Equation (1),[17]

$$O.C. = \frac{I_s - I_f}{I_s + I_f}, \tag{1}$$

where I_s and I_f are the intensities of the reflected light from the substrate and the flake, respectively. The O.C. is a measurable quantity that can be modelled using the Fresnel law for interference, depending on the thicknesses and the complex refractive indexes of the materials of the interfaces according to the following Equations (2) and (3).[7,18,19]

$$I_s = \left|\frac{r_{02} + r_{23}e^{-2i\phi 2}}{1 + r_{02}r_{23}e^{-2i\phi 2}}\right|^2, \tag{2}$$

$$I_f = \left|\frac{r_{01} + r_{12}e^{-2i\phi 1} + r_{23}e^{-2i(\phi 1+\phi 2)} + r_{01}r_{12}r_{23}e^{-2i\phi 2}}{1 + r_{12}r_{23}e^{-2i\phi 2} + r_{01}r_{12}e^{-2i\phi 1} + r_{01}r_{23}e^{-2i(\phi 1+\phi 2)}}\right|^2. \tag{3}$$

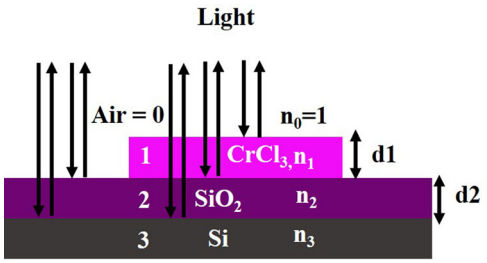

FIGURE 1 Schematic diagram of light incidence over three-interface system at 90° incident angle

Here, r_{jk} is defined as relative refractive index of two adjacent (j and k) materials as in Equation (4):

$$r_{jk} = \frac{n'_j - n'_k}{n'_j + n'_k}, \tag{4}$$

being $n'_j(\lambda) = n_j - i\kappa_j$ the complex refractive index of the j-th material.[19]

And, where

$$\phi_j = \frac{2\pi n_j d_j cos(\theta_j)}{\lambda} \tag{5}$$

is the phase shift introduced when the light passes through each medium (j), λ and d, respectively, being the wavelength of the radiation and the thickness of the material. In our particular case, the 0, 1, 2 and 3 correspond, respectively, to the air, $CrCl_3$, SiO_2 and Si. In every case, the Si layer is considered semi-infinite.[18,19]

3 | EXPERIMENTAL DETAILS

$CrCl_3$ crystals were grown and characterized as in Ref. 26 Experimental details of the preparation of the exfoliated samples can be taken from a previously published work.[25] In particular $CrCl_3$ showed to have longer degradation times of other tri-halides, another reason of interest for its investigation.[25] Layer-dependent experimental O.C. values have been fitted using a nonlinear fit model with n, k and λ as fitting parameters in a theoretical O.C. The values are calculated from Equations (1), (2) and (3) by considering the SiO_2 refractive index value equal to 1.5 with zero extinction coefficient. Such value has been considered, to a first approximation, wavelength independent.

The UV-Vis absorbance spectra were recorded by using Cary 8454 diode array spectrometer (Agilent Technologies, Santa Clara, CA, USA) with Agilent ChemStation software at room temperature within the range of 190–1100 nm wavelength.[27] The measurements were done at fast scan speed with a 0.9 nm sampling interval of the diode

array over 190–1100 nm wavelength range and 1 nm bandwidth slit.

The glass slides were being used as substrate and samples were mounted at the bottom of glass slides with the help of scotch tape, this whole system was set in a home-build sample support to perform the measurements. The mentioned system is shown in Figure S1. Prior to $CrCl_3$ measurements, we scanned the scotch tape wrapped glass slide to see the light absorbed through the scotch tape. The scotch tape did not show any absorbance and the spectra were completely flat (see Figure S2). Afterward, we recorded the spectra on $CrCl_3$ bulk and exfoliated one.

4 | RESULTS AND DISCUSSION

To investigate the effective wavelength range, we performed the UV-Vis spectroscopy on bulk as well as on exfoliated $CrCl_3$. Figure 2 shows the room temperature UV-Vis and NIR absorption spectra of bulk and cleaved $CrCl_3$ through black and red lines, respectively. Samples used for the experiment were presented in the inset of Figure 2(A) where two broad absorbance peaks were clearly observed at wavelengths 533 nm and 757 nm and at 530 nm and 729 nm for bulk and cleaved samples, respectively. The intensity of bulk $CrCl_3$ was higher than that of the exfoliated one because of the thickness and size of the sample (Figure S1). Figure 2(B) shows the data for both samples normalized to enhance the shape difference from the bulk counterpart to thin specimens. The two main features of the absorption edge come from the p-type valence band to quasi-localized d states.[28] Interestingly, the spectrum recorded from the exfoliated flakes is showing multiple kinks, while going through visible wavelength range. Spectrum contains three clear kinks at 500 nm, 530 nm and 559 nm. In Figure 2(C), the spectrum started to sharpen the curve from 500 nm wavelength and achieved a peak at 530 nm. Afterward the spectrum started to go down until 570 nm wavelength with a cone-shaped spectrum. The origin of the kinks are evidently related to the 2D nature of the sample. Though the UV-Vis technique cannot be tuned to individual flakes with their own layer thickness because of the small lateral sample size, we aim at establishing a correlation between the contrast and the absorption/interference properties of the thin $CrCl_3$.

We already reported the O.C. for few layers of $CrCl_3$ in Ref. 25 In this study, to make a direct correlation between the experimental data with theory, we have employed a non-linear fitting programme based on Fresnel's interference quantitative comparison.

To validate our Fresnel's interference–based model on other well-known 2D reference materials, that is, graphene, MoS_2 and CrI_3, we have performed a parallel

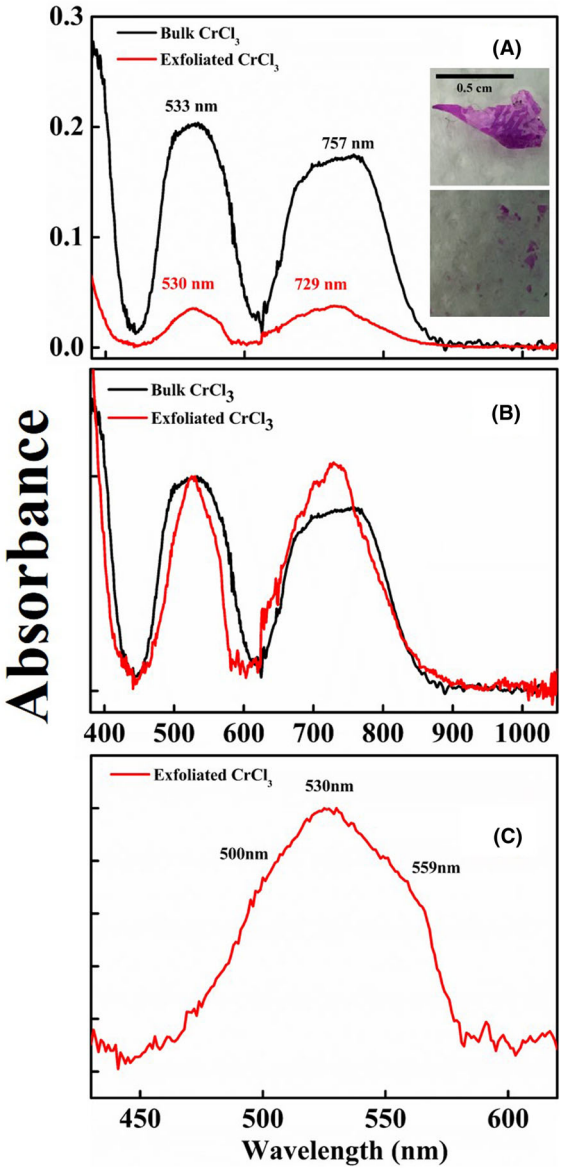

FIGURE 2 UV-visible absorbance spectra of $CrCl_3$ on glass substrate: (A) spectra for bulk (black) and exfoliated (red) $CrCl_3$. The images of used samples are presented in the inset. (B) Comparison of shape of bulk and exfoliated samples after normalization. (C) Absorption spectrum of exfoliated flakes are within 440–620 nm wavelength range

study and the results have been presented in the Supporting Information in Figure S3. We reported the best fitting parameters for all three materials taken from literature, which are also presented in the Supporting Information. In our case, we fitted the O.C. data for $CrCl_3$ on 270 nm and 285 nm SiO_2/Si substrates. In most of the cases, the refractive index is a slowly varying function with respect to the wavelength. This latter point justifies our mean value approach, by using constant optical parameters. In Figure 3, we presented together with the best fit curves of the experimental contrast, obtained by optimizing the three

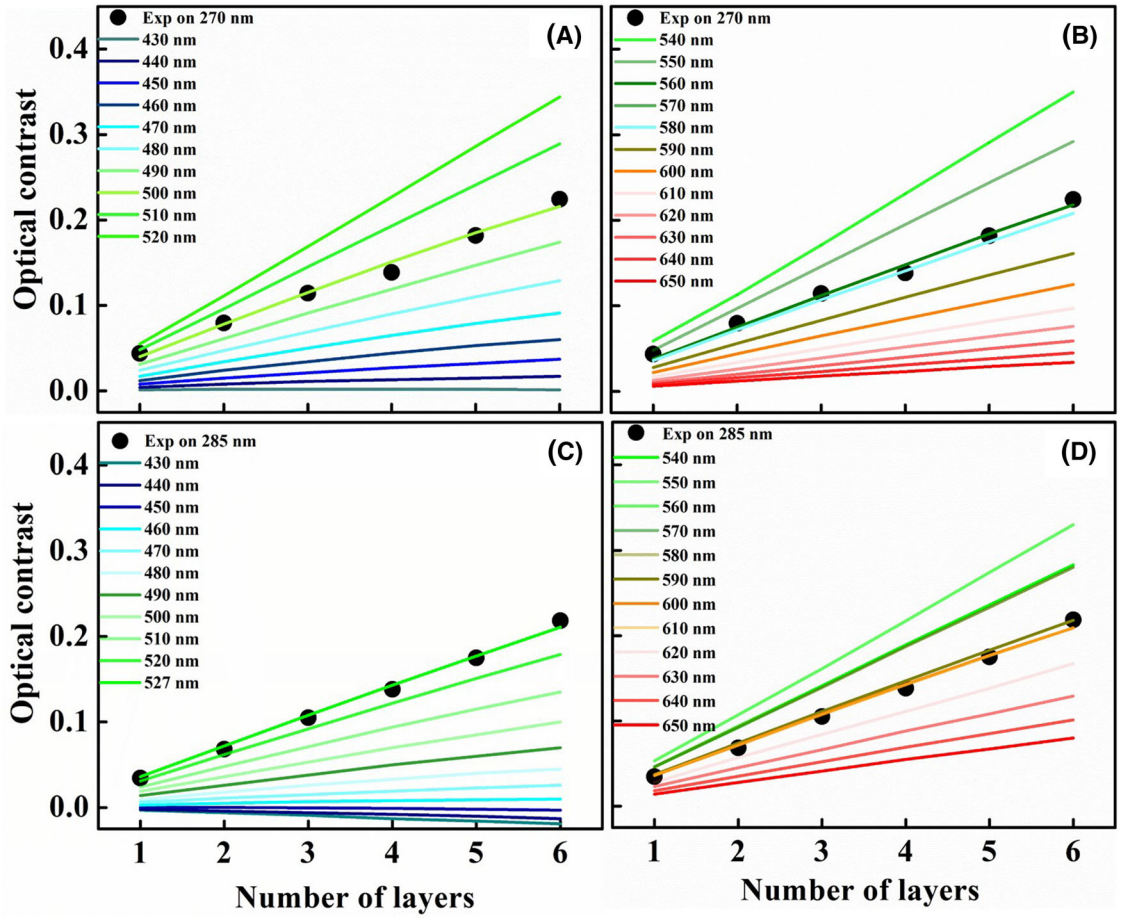

FIGURE 3 The simulated optical contrast (O.C.) for different number of layers (one to six) of $CrCl_3$ by changing the wavelength interval on different SiO_2 thicknesses on top of Si wafer, that is, 270 nm (upper panels) and 285 nm (lower panels). The circles represent the experimental values of the O.C. The thick lines in (A,C) represent the simulated data from 430 to 530 nm wavelength; while in (B,D) we report simulated contrast for the wavelength range from 540 to 650

parameters (λ, n and k), also the calculations of theoretical contrast at other wavelengths spanning the whole experimental range.

The black circles show the experimental O.C. data for 270 nm (upper panels (A,B)) and 285 nm (lower panels (C,D)) SiO_2/Si substrates, respectively. We calculated the contrast value for one to six layers by varying the wavelength within 430–520 nm and 540–650 nm range, respectively, for left and right panels. Each wavelength corresponds to a different colour of line. In Figure 3(A) the light green curve, which corresponds to 500 nm wavelength illumination, befits the experimental data. While most of the wavelengths make the contrast near to zero. Wavelengths from 560 nm to 580 nm befitted the experimental data as well. A similar study was performed on 285 nm SiO_2/Si substrate, as the O.C. is slightly different from the other substrates. The analysis also occurred in two intervals, Figure 3(C) corresponds to 430–527 nm wavelength range and Figure 3(D) covers the illumination wavelength from 530 nm to 650 nm. Figure 3(C) clearly shows that 527 nm illumination wavelength fits the experimental data and Figure 3(D) shows that experimental O.C. was fitted perfectly by 590 nm and 600 nm illumination wavelengths. Based on the results, the highest visibility of $CrCl_3$ thin flakes was obtained within green–yellow illumination wavelength range.

We stress that the best fitted O.C. curves are obtained as a fitting search over the full parameter space while the other curves without good agreement with the experimental data are simple simulations. While keeping the full visible wavelength range the best fitted data give the optical constants as well as effective wavelengths for both substrates (the values are presented in Table 1).

These perfectly fitted data correlate with absorption spectra. The experimental O.C. data resonate at particular wavelengths and almost overlap to the theoretical O.C. values. From literature, we know that the extinction coefficient part is equally important as it changes the O.C. of materials by absorption and interference of light, which may lead to the destructive interference. In our case, three

TABLE 1 The optical constants values at different SiO_2 thickness substrates

SiO_2 thickness (nm)	One layer thickness (nm)	*n*	*k*	Wavelength (nm)
270	0.65	1.1 ± 0.2	1.1 ± 0.1	560
285	0.65	1.1 ± 0.2	1.1 ± 0.1	527

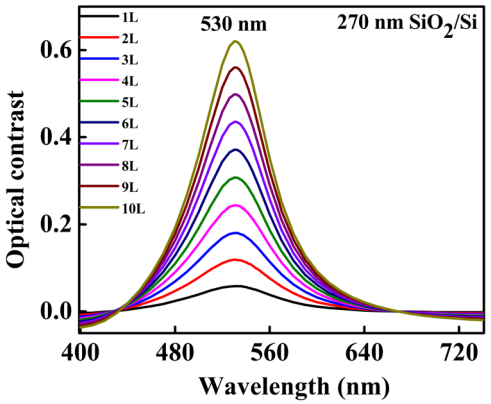

FIGURE 4 Normal incidence theoretical optical contrast spectra of $CrCl_3$ flakes for 1–10 layers on 270-nm-thick SiO_2 on Si substrate for visible wavelength range

noticeable kinks are supposed to influence the O.C. value by producing a resonance within visible wavelength range, due to this more intense absorption.

Figure 4 shows the theoretical contrast spectra of $CrCl_3$ for 1–10 layers on 270 nm SiO_2/Si substrates. The spectra have been taken across the full range of visible light (400–740 nm) calculated by Equation (1) in numerical simulation on 270 nm SiO_2/Si substrate, showing the maximum visibility. The contrast spectrum of single monolayer was centred at 530 nm wavelength.

Noteworthy, the numerical simulation of the O.C., relying on almost constant optical parameters, could miss modulation induced by the presence of absorption kinks. In this manner, Figures 2, 3 and 4 are not in conflict with each other. We also reported in the Supporting Information (Figure S4) the simulation in the case of MoS_2 done by a finite element time–dependent programme, using a built-in refractive index function; the latter showing that the nominally exact contrast calculations are consistent with the presence of a resonance region around the mean value of the wavelength determined by the fit (Figure 4).

5 | CONCLUSIONS

We have demonstrated the importance of O.C. to identify the thickness of $CrCl_3$ 2D material. In case of CrX_3 (X = Cl, Br and I), the layers are not sensitive enough to be detected under Raman spectroscopy at room temperature. Even near Curie temperature a very small shift (2–3 cm^{-1}) occurs by down-scaling the thickness of the materials. In this situation, O.C. measurements play a critical role for the layers' number identification. Our experimental data were matched with theoretical calculations by using Fresnel's equations. As we used white light illumination for experimental analysis, the study allows to know the most sensitive region of the whole visible range to observe the highest contrast for each material. A nonlinear simulation program demonstrates the viability of the method by testing the graphene, MoS_2 and CrI_3. From the simulations, we successfully extracted the effective wavelength along with complex refractive index (1.1–1.1i) for 1-6L $CrCl_3$. Moreover, the UV-Vis absorption spectra confirmed the highly sensitive wavelength region for the material. From the experimental and theoretical analysis, we found that 270 nm SiO_2/Si substrate showed the highest visibility among all used thicknesses of SiO_2 capping layers. A quantitative experimental study is needed to maximize the contrast of $CrCl_3$ layers on SiO_2/Si (with different thicknesses of SiO_2) or other substrates. We believe that this study will provide a quick and accurate approach to detect the thin layers of any 2D materials, without posing restrictions on the light source used in the optical microscope contrast measurements.

ORCID

Roberto Gunnella https://orcid.org/0000-0003-4739-6375
Marco Zannotti https://orcid.org/0000-0003-2527-9856

REFERENCES

1. Novoselov, K. S., Jiang, D., Schedin, F., Booth, T. J., Khotkevich, V. V., Morozov, S. V., & Geim, A. K. (2005). Two-dimensional atomic crystals. *Proceedings of the National Academy of Sciences*, *102*(30), 10451–10453.
2. Mounet, N., Gibertini, M., Schwaller, P., Campi, D., Merkys, A., Marrazzo, A., Sohier, T., Castelli, I. E., Cepellotti, A., Pizzi, G., & Marzari, N. (2018). Two-dimensional materials from high-throughput computational exfoliation of experimentally known compounds. *Nature Nanotechnology*, *13*(3), 246–252.
3. Mak, K. F., Lee, C., Hone, J., Shan, J., & Heinz, T. F. (2010). Atomically thin MoS 2: A new direct-gap semiconductor. *Physical Review Letters*, *105*(13), 136805.
4. Yi, Y., Chen, Z., Yu, X.-F., Zhou, Z.-K., & Li, J. (2019). Recent advances in quantum effects of 2D materials. *Advanced Quantum Technologies*, *2*(5-6), 1800111.
5. Mueller, T., & Malic, E. (2018). Exciton physics and device application of two-dimensional transition metal dichalcogenide semiconductors. *npj 2D Materials and Applications*, *2*(1), 1–12.

6. Novoselov, K., Mishchenko, A., Carvalho, A., & Neto, A. C. (2016). 2D materials and van der Waals heterostructures. *Science*, *353*(6298).
7. Huang, B., Clark, G., Navarro-Moratalla, E., Klein, D. R., Cheng, R., Seyler, K. L., Zhong, D., Schmidgall, E., McGuire, M. A., Cobden, D. H., Yao, W., Xiao, D., Jarillo-Herrero, P., & Xu, X. (2017). Layer-dependent ferromagnetism in a van der Waals crystal down to the monolayer limit. *Nature*, *546*(7657), 270–273.
8. Zeng, Z., Yin, Z., Huang, X., Li, H., He, Q., Lu, G., Boey, F., & Zhang, H. (2011). Single-layer semiconducting nanosheets: High-yield preparation and device fabrication. *Angewandte Chemie*, *123*(47), 11289–11293.
9. Klein, D. R., MacNeill, D., Lado, J. L., Soriano, D., Navarro-Moratalla, E., Watanabe, K., Taniguchi, T., Manni, S., Canfield, P., Fernández-Rossier, J., & Jarillo-Herrero, P. (2018). Probing magnetism in 2D van der Waals crystalline insulators via electron tunneling. *Science*, *360*(6394), 1218–1222.
10. Cai, X., Song, T., Wilson, N. P., Clark, G., He, M., Zhang, X., Taniguchi, T., Watanabe, K., Yao, W., McGuire, M. A., Cobden, D. H., & Xu, X. (2019). Atomically thin CrCl3: An in-plane layered antiferromagnetic insulator. *Nano Letters*, *19*(6), 3993–3998.
11. Liu, J., Sun, Q., Kawazoe, Y., & Jena, P. (2016). Exfoliating biocompatible ferromagnetic Cr-trihalide monolayers. *Physical Chemistry Chemical Physics*, *18*(13), 8777–8784.
12. Pollini, I., & Spinolo, G. (1970). Intrinsic optical properties of CrCl3. *Physica Status Solidi (b)*, *41*(2), 691–701.
13. Li, X., Cai, W., An, J., Kim, S., Nah, J., Yang, D., Piner, R., Velamakanni, A., Jung, I., Tutuc, E., Banerjee, S. K., Colombo, L., &, Ruoff, R. S. (2009). Large-area synthesis of high-quality and uniform graphene films on copper foils. *Science*, *324*(5932), 1312–1314.
14. Li, X., Magnuson, C. W., Venugopal, A., An, J., Suk, J. W., Han, B., Borysiak, M., Cai, W., Velamakanni, A., Zhu, Y., Fu, L., Vogel, E. M., Voelkl, E., Colombo, L., & Ruoff, R. S. (2010). Graphene films with large domain size by a two-step chemical vapor deposition process. *Nano Letters*, *10*(11), 4328–4334.
15. Ramakrishna Matte, H., Gomathi, A., Manna, A. K., Late, D. J., Datta, R., Pati, S. K., & Rao, C. (2010). MoS2 and WS2 analogues of graphene. *Angewandte Chemie International Edition*, *49*(24), 4059–4062.
16. Frindt, R. (1966). Single crystals of MoS_2 several molecular layers thick. *Journal of Applied Physics*, *37*(4), 1928–1929.
17. Ottaviano, L., Palleschi, S., Perrozzi, F., D'Olimpio, G., Priante, F., Donarelli, M., Benassi, P., Nardone, M., Gonchigsuren, M., Gombosuren, M., Lucia, A., Moccia, G., & Cacioppo, O. A. (2017). Mechanical exfoliation and layer number identification of MoS_2 revisited. *2D Materials*, *4*(4), 045013.
18. Bing, D., Wang, Y., Bai, J., Du, R., Wu, G., & Liu, L. (2018). Optical contrast for identifying the thickness of two-dimensional materials. *Optics Communications*, *406*, 128–138.
19. Blake, P., Hill, E., Castro Neto, A., Novoselov, K., Jiang, D., Yang, R., Booth, T., & Geim, A. (2007). Making graphene visible. *Applied Physics Letters*, *91*(6), 063124.
20. Ni, Z., Wang, H., Kasim, J., Fan, H., Yu, T., Wu, Y. H., Feng, Y., & Shen, Z. (2007). Graphene thickness determination using reflection and contrast spectroscopy. *Nano Letters*, *7*(9), 2758–2763.
21. Zhang, X., Kawai, H., Yang, J., & Goh, K. E. J. (2019). Detecting MoS_2 and $MoSe_2$ with optical contrast simulation. *Progress in Natural Science: Materials International*, *29*(6), 667–671.
22. Weber, J., Calado, V., & Van De Sanden, M. (2010). Optical constants of graphene measured by spectroscopic ellipsometry. *Applied Physics Letters*, *97*(9), 091904.
23. Ermolaev, G. A., Yakubovsky, D. I., Stebunov, Y. V., Arsenin, A. V., & Volkov, V. S. (2020). Spectral ellipsometry of monolayer transition metal dichalcogenides: Analysis of excitonic peaks in dispersion. *Journal of Vacuum Science & Technology B, Nanotechnology and Microelectronics: Materials, Processing, Measurement, and Phenomena*, *38*(1), 014002.
24. Hsu, C., Frisenda, R., Schmidt, R., Arora, A., De Vasconcellos, S. M., Bratschitsch, R., van der Zant, H. S., & Castellanos-Gomez, A. (2019). Thickness-dependent refractive index of 1L, 2L, and 3L MoS_2, MoSe2, WS2, and WSe2. *Advanced Optical Materials*, *7*(13), 1900239.
25. Kazim, S., Ali, M., Palleschi, S., D'Olimpio, G., Mastrippolito, D., Politano, A., Gunnella, R., Di Cicco, A., Renzelli, M., Moccia, G., Cacioppo, O. A., Alfonsetti, R., Strychalska-Nowak, J., Klimczuk, T., Cava, R. J., & Ottaviano, L. (2020). Mechanical exfoliation and layer number identification of single crystal monoclinic $CrCl_3$. *Nanotechnology*, *31*, 395706.
26. Serri, M., Cucinotta, G., Poggini, L., Serrano, G., Sainctavit, P., Strychalska-Nowak, J., Politano, A., Bonaccorso, F., Caneschi, A., Cava, R. J., Sessoli, R., Ottaviano, L., Klimczuk, T., Pellegrini, V., & Mannini, M. (2020). Enhancement of the magnetic coupling in exfoliated CrCl3 crystals observed by low-temperature magnetic force microscopy and X-ray magnetic circular dichroism. *Advanced Materials*, *32*, 2000566.
27. D'Amato, C. A., Giovannetti, R., Zannotti, M., Rommozzi, E., Minicucci, M., Gunnella, R., & Di Cicco, A. (2018). Band gap implications on nano-TiO_2 surface modification with ascorbic acid for visible light-active polypropylene coated photocatalyst. *Nanomaterials*, *8*(8), 599.
28. Pollini, I. (1998). Electron correlation and hybridization in chromium compounds. *Solid State Communication*, *106*(8), 549.

SUPPORTING INFORMATION

Additional supporting information may be found online in the Supporting Information section at the end of the article.

How to cite this article: Kazim S, Gunnella R, Zannotti M, et al. Determination of the refractive index and wavelength-dependent optical properties of few-layer $CrCl_3$ within the Fresnel formalism. *Journal of Microscopy*. 2021;*283*:145–150. https://doi.org/10.1111/jmi.13015